

## **Numerical modelling of anisotropy of Otaniemi Clay**

Heiko P. Neher & Christoph Sterr

*Institute of Geotechnical Engineering, University of Stuttgart, Germany*

Sophie Messerklinger

*Institute for Geotechnical Engineering, Swiss Federal Institute of Technology, Zurich, Switzerland*

Mirva Koskinen

*Department of Civil and Environmental Engineering, Helsinki University of Technology, Finland*

**ABSTRACT:** The performance of four constitutive models is compared with the results of triaxial tests on natural Otaniemi Clay. The conducted triaxial tests demonstrate the anisotropic behaviour of Otaniemi Clay. Two models are formulated in the classical framework of elasto-plasticity. One of them is an elasto/viscoplastic model and the other one has a rotational hardening rule. The other two models are based on the multilaminate framework. One of the multilaminate type models is an elasto/viscoplastic model as well. The results show a satisfactory match for most of the tests for all models. It is also obvious that the models with anisotropic formulations (model with rotational hardening rule and multilaminate type models) perform overall better than the isotropic model. Moreover, it seems that for this kind of tests modelling viscosity is not that important.

### **1 INTRODUCTION AND CONSTITUTIVE LAWS**

The modelling of anisotropic behaviour of soils is important for many engineering applications. Therefore, different constitutive models have been proposed to account for the anisotropy of soils. In the present paper the anisotropy of a natural clay (Otaniemi clay) exhibited in triaxial tests will be considered. The test results will be compared to model simulations with four different constitutive models. A brief introduction into the models is given in this section. The sign convention used assumes compression positive and all stresses and parameters are effective stress parameters.

The first model is an anisotropic elasto-plastic model called S-CLAY1. The second one is an isotropic elasto/viscoplastic model named Soft-Soil-Creep (SSC). The third model, called Multilaminate-Creep (MLC) model, and the fourth model, called Multilaminate Model for Clay (MMC) are based on the multilaminate framework that accounts for anisotropy. The MLC model is an elasto/viscoplastic model like the SSC model, and the MMC model is an elasto-plastic model.

#### *1.1 S-CLAY1 model*

The initial anisotropy in the S-CLAY1 model is described by the initial orientation of the yield surface in the three dimensional stress space. A rotational hardening component controls the induced anisotropy during loading. In the triaxial stress space for a cross-anisotropic sample, the yield surface of the S-CLAY1 model can be expressed in terms of mean stress  $p$  and deviator stress  $q$ .

$$f = (q - \alpha p)^2 - (M^2 - \alpha^2)(p_m - p)p = 0 \quad (1)$$

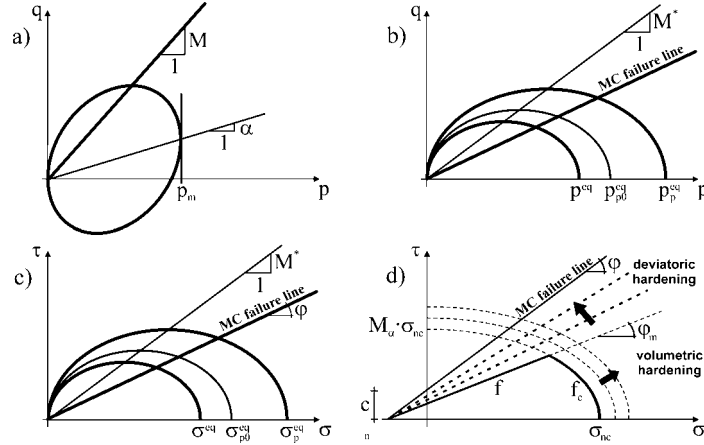


Figure 1. a) The yield surface in  $p$ - $q$ -space for the S-CLAY1 model; b) Plot of the SSC model in  $p$ - $q$ -space; c) Plot of the MLC model on a plane; d) Yield surfaces on a plane for the MMC model.

In Eq. (1)  $M$  is the value of the stress ratio  $\eta = q/p$  at critical states,  $\alpha$  defines the orientation of the yield surface and  $p_m$  defines the size of the yield surface (Fig. 1a). The elastic behaviour is assumed to be isotropic with a formulation that is identical to the one used in the Modified Cam Clay (MCC) model (Roscoe & Burland 1968). Likewise, an associated flow rule is assumed.

The S-CLAY1 model incorporates two hardening laws. One concerns changes in the size of the yield surface and the other concerns changes in the orientation of the yield surface. The former is the same as used in the MCC model, and the latter can be expressed as

$$d\alpha = \mu \left[ \left( \frac{3\eta}{4} - \alpha \right) \langle d\varepsilon_v^p \rangle + \beta \left( \frac{\eta}{3} - \alpha \right) |d\varepsilon_d^p| \right] \quad (2)$$

where  $d\varepsilon_v^p$  is the plastic volumetric strain increment and  $d\varepsilon_d^p$  is the plastic deviatoric strain increment. The parameter  $\mu$  controls the rate at which  $\alpha$  heads towards its target value. The parameter  $\beta$  characterises the relative effectiveness of volumetric and deviatoric strains in rotating the yield surface.  $\mu$  and  $\beta$  are additional parameters in comparison to the MCC model. The determination of these parameters as well as the initial state (size and inclination of the yield surface), is discussed in Näätänen, Wheeler, Karstunen & Lojander (1999). A detailed description of the S-CLAY1 model is given in Wheeler, Näätänen, Karstunen & Lojander (2003).

## 1.2 Soft-Soil-Creep model

The SSC model is based on the MCC model. However, there are two main differences. The Mohr-Coulomb (MC) criterion is used to describe failure and viscous soil behaviour is included.

The description of the model in the triaxial stress space allows expressing any stress state by a point lying on a surface that can be represented as an ellipse in the  $p$ - $q$ -plane. The apex of the ellipse is located on a line with the inclination  $M^*$ . However this line is selected in such a manner that under oedometric loading conditions the earth pressure at rest  $K_0$  is predicted realistically. Eq. (3) defines an equivalent stress  $p^{eq}$ , which represents the actual stress state (see Fig. 1b). Moreover, an equivalent pre-consolidation pressure  $p_p^{eq}$  is introduced, which is a function of the accumulated volumetric creep strain and the initial equivalent pre-consolidation pressure  $p_{p0}^{eq}$ .

$$p^{eq} = p + \frac{q}{M^* p} \quad \text{and} \quad p_p^{eq} = p_{p0}^{eq} \cdot \exp\left(\frac{\Delta\varepsilon_v^{cr}}{\lambda^* - \kappa^*}\right) \quad (3)$$

In the SSC model the MC-failure line is fixed, but the cap (ellipse with  $p_p^{eq}$ ) moves due to volumetric creep strain. By assuming an associated flow rule one can easily calculate the total creep strain rate as defined in Eq. (4), where  $\kappa^*$ ,  $\lambda^*$  and  $\mu^*$  are the modified swelling, compression and creep index, respectively.  $\tau_t$  is a time constant that is set to one day.

$$\dot{\boldsymbol{\varepsilon}}^{cr} = \frac{1}{\alpha} \dot{\varepsilon}_v^{cr} \cdot \frac{\partial p^{eq}}{\partial \boldsymbol{\sigma}} = \frac{1}{\alpha} \frac{\mu^*}{\tau_t} \left( \frac{p^{eq}}{p_p^{eq}} \right)^{\frac{\lambda^* - \kappa^*}{\mu^*}} \cdot \frac{\partial p^{eq}}{\partial \boldsymbol{\sigma}} \quad \text{with} \quad \alpha = \frac{\partial p^{eq}}{\partial p} \quad (4)$$

The elastic behaviour is assumed to be isotropic with a stress dependent stiffness similar to the MCC model. For further details of the model the reader is referred to Vermeer & Neher (1999). A description including cohesion is given in Neher, Wehnert & Bonnier (2001).

### 1.3 Multilaminate type models

The multilaminate framework was introduced by Zienkiewicz & Pande (1977), Pande & Sharma (1983) and Pietruszczak & Pande (1987) for rocks and soil. The physical model is a solid block of homogeneous isotropic elastic material, which is intersected by an infinite number of randomly oriented planes. The deformation behaviour of such a material block is obtainable by a description of the sliding phenomenon under a current effective normal and shear stress component on the planes ( $\sigma_n$ ,  $\tau$ ) and the opening/closing of the inter-boundary gap between two contact planes. The infinite number of planes yields to a homogeneous material behaviour of the block that is no longer elastic.

The local stress vector  $\bar{\boldsymbol{\sigma}}_i$  on contact plane  $i$  can be derived from the global stress vector  $\boldsymbol{\sigma}$  by stress transformation, see Eq. (5).

$$\bar{\boldsymbol{\sigma}}_i = [\mathbf{T}]_i^T \cdot \boldsymbol{\sigma} \quad (5)$$

The stress-strain relations are formulated locally on the planes (microscopic level), except for the elastic part, which is calculated on the global (or macroscopic) level. The global behaviour is obtained by integration of the inelastic contributions from each contact plane and summing it up with the global elastic part. The integration over an infinite number of planes is numerically replaced by an integration rule, which is a summation over  $n$  defined planes,

$$d\boldsymbol{\varepsilon}^p = \sum_{i=1}^n w_i \cdot [\mathbf{T}]_i \cdot d\lambda_i \cdot \frac{\partial \mathbf{g}}{\partial \bar{\boldsymbol{\sigma}}_i} \quad (6)$$

where  $d\lambda_i$  is the length of the local inelastic strain vector and  $\partial \mathbf{g} / \partial \bar{\boldsymbol{\sigma}}_i$  is its direction. The transformation matrix  $[\mathbf{T}]_i$  and the weight factor  $w_i$  are different for each plane.

In the simulations, an integration rule over  $n = 33$  planes per hemisphere (Bažant & Oh 1985) is used for both multilaminate type models. This integration rule seems to be sufficient for multilaminate models to get reliable results and to avoid excessive memory requirements. Moreover, it is assumed that all planes have the same properties, although this is not essential.

#### 1.3.1 Multilaminate-Creep model

The MLC model is an extension of the SSC model that incorporates anisotropy by using the multilaminate framework. The formulation of the creep strains is done on the microscopic level. Thus Eqs. (3) and (4) have to be modified for the conditions on a plane. The same accounts for the MC criterion. Therefore mean and deviatoric stresses are replaced by normal and shear stresses on a plane. The equivalent stress  $p^{eq}$ , the pre-consolidation pressure  $p_p^{eq}$  and the initial pre-consolidation pressure  $p_{p0}^{eq}$  are substituted by  $\sigma^{eq}$ ,  $\sigma_p^{eq}$  and  $\sigma_{p0}^{eq}$ , respectively, see Fig. 1c. Moreover, the normal creep strain on a plane replaces the volumetric creep strain. The same accounts for the strain rate, respectively. Thus Eq. (4) can be transformed to

$$\dot{\varepsilon}_i^{cr} = \frac{1}{\alpha} \dot{\varepsilon}_n^{cr} \cdot \frac{\partial \sigma^{eq}}{\partial \bar{\boldsymbol{\sigma}}_i} = \frac{1}{\alpha} \frac{\mu^*}{\tau_t} \left( \frac{\sigma^{eq}}{\sigma_p^{eq}} \right)^{\frac{\lambda^* - \kappa^*}{\mu^*}} \cdot \frac{\partial \sigma^{eq}}{\partial \bar{\boldsymbol{\sigma}}_i} \quad \text{with} \quad \alpha = \frac{\partial \sigma^{eq}}{\partial \sigma_n} \quad (7)$$

More information about the MLC model is given in Neher, Vermeer & Bonnier (2001) and Neher, Cudny, Wiltafsky & Schweiger (2002).

### 1.3.2 Multilaminate Model for Clay

The MMC model is based on the double hardening model proposed by Vermeer (1978) with slightly different formulations for the yield surfaces. Moreover, it has been modified to fit into the multilaminate framework. The MMC model has two yield surfaces (see Fig. 1d). A non-associated flow rule is used for the yield surface  $f$  whereas an associated flow rule is assumed for the yield surface  $f_c$ .

$$f = \tau - \sigma_n \tan \varphi_m - \frac{c \cdot \tan \varphi_m}{\tan \varphi} = 0 \quad \text{with} \quad \tan \varphi_m = \tan \varphi_i + (\tan \varphi - \tan \varphi_i) \frac{\varepsilon_\gamma^p}{A + \varepsilon_\gamma^p} \quad (8)$$

$$f_c = \frac{\sigma_n^2}{\sigma_{nc}^2} + \frac{\tau^2}{(M_\alpha \sigma_{nc})^2} - 1 = 0 \quad (9)$$

In Eq. 8  $\varphi_m$  and  $c$  are the mobilised friction angle and the cohesion, respectively. The mobilised friction angle  $\varphi_m$  increases with deviatoric hardening, which is controlled by plastic shear strains  $\varepsilon_\gamma^p$ , until the peak friction angle  $\varphi$  is reached. Parameter  $A$  controls the rate of deviatoric hardening,  $\varphi_i$  is the mobilised friction angle of the initial stress state,  $\sigma_{nc}$  represents the pre-consolidation stress state resulting from the loading history and  $M_\alpha \cdot \sigma_{nc}$  defines the shape of the elliptic yield surface  $f_c$ . A detailed description of the MMC model can be found in Wiltafsky, Messerklinger & Schweiger (2002).

## 2 OTANIEMI CLAY

Otaniemi clay is a very soft clay from southern Finland next to the Gulf of Finland. Some typical properties for Otaniemi clay are given in Table 1. The simulation results presented in this paper relate to drained triaxial tests performed on undisturbed natural samples from a depth of 3.5 to 4.7 m. A full description of the whole testing programme on Otaniemi clay carried out at Helsinki University of Technology to investigate the anisotropic behaviour of clay is given in Wheeler, Nääätänen, Karstunen & Lojander (2003) and Toivanen (1999). The tests involved two loading and unloading cycles with different stress ratios  $\eta = q/p$ . Table 2 summarizes the tests on Otaniemi clay simulated in this paper. The tests CAD 2261 and CAD 2251 are both compression tests, where for the former the first loading lays above the  $K_\theta$ -path and for the latter first loading follows approximately the  $K_\theta$ -path. The test CID 2403 is first loaded isotropically, thus the stress ratio between the confining and the axial pressure is  $K = \sigma_3/\sigma_1 = 1$ . The extension test has the reference CAE 2496, and the  $K$ -value in this case is over 1.

Table 1. Parameters of Otaniemi clay.

Property	Notation	Value
clay sized fraction	Cl [%]	65 – 83
specific density	$\rho_s$ [g/cm <sup>3</sup> ]	2.76 - 2.80
water content	w [-]	84 – 130
liquid limit	w <sub>L</sub> [-]	80 – 111
plastic limit	w <sub>P</sub> [-]	26 – 29
organic content	Hm [%]	0.0 - 0.7
undrained shear strength	$c_u$ [kN/m <sup>2</sup> ]	6 – 9
sensitivity	S <sub>t</sub> [-]	7 – 14

Table 2. Simulated triaxial tests on Otaniemi clay.

Test reference	Depth [m]	w [%]	$e_0$ [-]	$\eta_1$ [-]	$\eta_2$ [-]
CAD 2261	4.03 - 4.14	94.8	2.62	0.9	0.1
CAD 2251	4.20 - 4.31	92.0	2.51	0.6	0.1
CID 2403	3.62 - 3.73	120.2	3.30	0.0	0.4
CAE 2496	4.20 - 4.31	93.8	2.57	-0.3	0.1

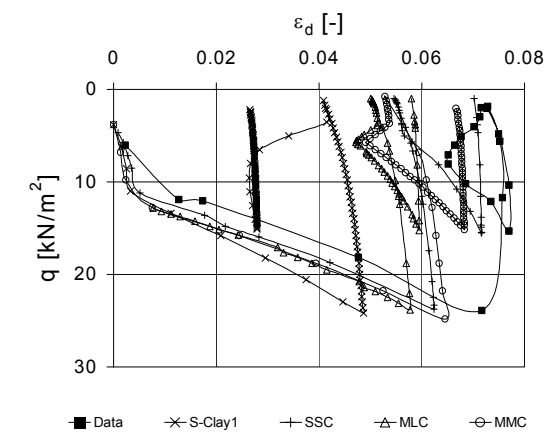
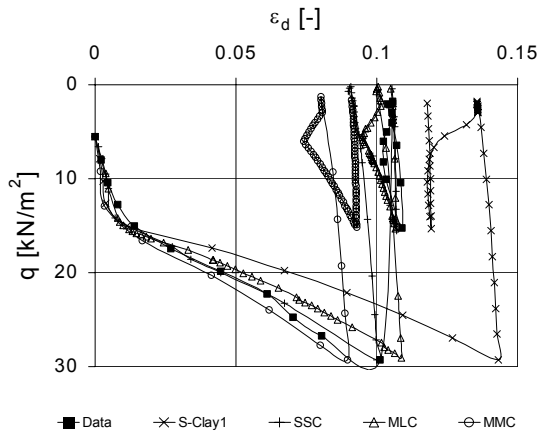
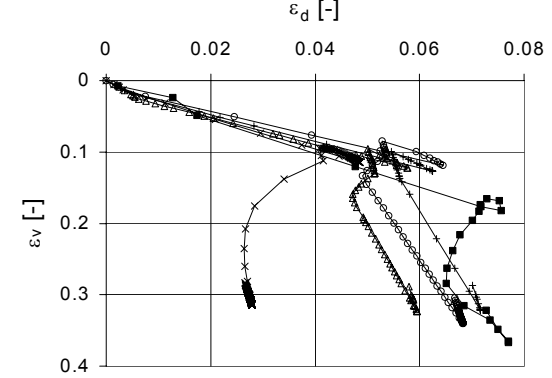
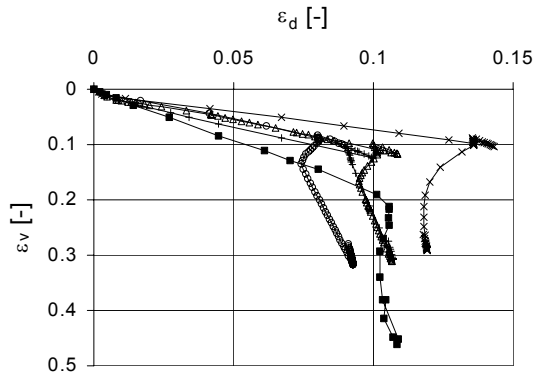
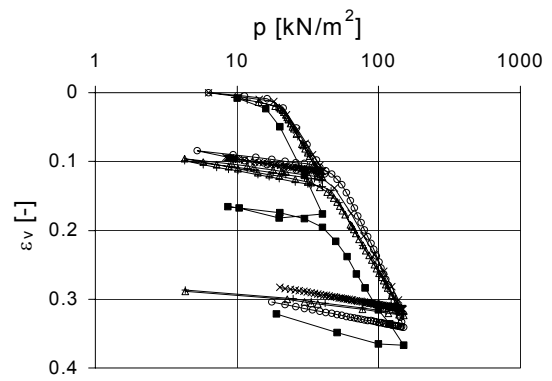
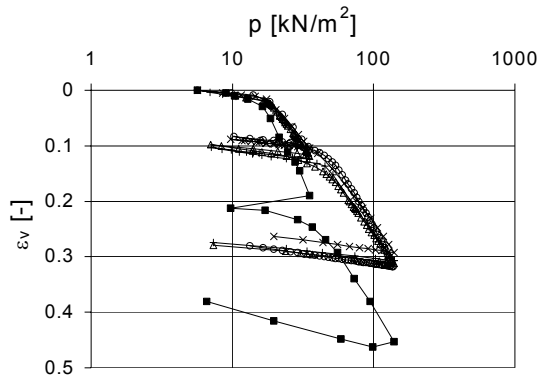


Figure 2. CAD 2261 test results and simulations.

Figure 3. CAD 2251 test results and simulations.

The Poisson's ratio for un-/reloading for all models is  $\nu_{ur} = 0.2$ . The MC parameters are the friction angle  $\varphi = 27.7^\circ$ , the dilatancy angle  $\psi = 0^\circ$  and the cohesion  $c = 0$ . The other parameters used are given in Table 3.

Table 3. Input parameters for the used models.

Model	$M/M^*$	$\kappa/\kappa^* [-]$	$\lambda/\lambda^* [-]$	$\mu^* [-]$	$\mu [-]$	$\alpha [-]$	$\beta [-]$	$A [-]$
S-CLAY1	1.1 / -	0.04 / -	0.44 / -	-	20	-	0.67	-
SSC	- / 1.5	- / 0.015	- / 0.15	0.0035	-	-	-	-
MLC	- / 0.578	- / 0.015	- / 0.15	0.0035	-	-	-	-
MMC	-	0.04 / -	0.44 / -	-	-	0.67	-	0.001

### 3 COMPARISON OF TEST RESULTS AND NUMERICAL SIMULATIONS

The initial stress state for all four models was achieved by simulating an anisotropic  $K_0$ -path loading up to the in situ stress conditions of the soil samples followed by an unloading up to the starting condition of the drained triaxial tests. This process created the initial anisotropy for the simulations of the drained triaxial tests with the two loading/unloading cycles. The Figs. 2 to 5 show the comparisons between the different simulations and the test data. The calculations with the S-CLAY1 and the MMC model were performed by Messerklinger (2000). Sterr (2002) has done the analyses with the SSC and the MLC model. In Figs. 2 to 5, the top diagrams show the semi-logarithmic mean effective stress-volumetric strain plots. The second ones show the volumetric strains in relation to the deviatoric strains, whereas the third ones illustrate the deviatoric stress-deviatoric strain behaviour.

The performances of all models are approximately the same for the compression tests in a semi-logarithmic stress-volumetric strain plot. Some minor differences between the elasto/viscoplastic and the other models are shown in CID 2403 and the differences increase for CAE 2496. Based on these plots it is obvious, that viscous effects play only a small role in the tests. This is probably due to the selection of the loading rate. In fact all tests were performed with small stress increments ( $\Delta\sigma_3 = 2$  to  $4$  kN/m<sup>2</sup> for the first loading) loaded every 1 to 3 days, so that the samples were fully consolidated under each loading step. The next increment was applied shortly after consolidation had finished, thus not much time for creep was left.

The predicted volumetric strain is half of the observed volumetric strain in test CID 2403. This is probably due to the fact that for all simulations the same parameters were used despite the sample in this test being softer than the other samples, as indicated by the higher water content and initial void ratio  $e_0$  (Table 2). Furthermore, the values of  $\lambda$  and  $\lambda^*$  used in simulations were determined from an isotropic test. Using values of  $\lambda$  and  $\lambda^*$  corresponding to  $K_0$ -conditions would improve the predictions of volumetric strains significantly with all models, because they represent the average for most stress paths (Koskinen, Karstunen & Wheeler 2002).

With the  $\lambda$  and  $\lambda^*$  values adopted, it seems that an anisotropic formulation has no advantages in predicting volumetric strains for these kinds of tests. However, looking at the deviatoric strain-volumetric strain diagrams, it is clear that for the overall performance accounting for anisotropy is necessary. Especially the development of deviatoric strains during the isotropic loading cycle ( $\eta_1 = 0.0$ ) in test CID 2403 cannot be modelled with an isotropic formulation, see Fig. 4. The SSC model predicts deviatoric strains only when the second loading path ( $\eta_2 = 0.4$ ) is considered.

The direction of the (plastic) strains is expressed in the deviatoric strain-volumetric strain diagrams. The correctness of the flow rule used in each model can be checked easily even if the volumetric strain is not predicted correctly: the inclination of the curves (data and model) in a deviatoric strain-volumetric strain diagram are similar, if the flow rule of a model is appropriate. In test CAD 2261 the strain gradient of first loading is overpredicted at least by a factor of 1.5 by all models, whereas for test CAD 2251 the overprediction for first loading is very small. In the second loading stage of both tests, the pattern of straining is predicted best by S-CLAY1 model even though all models perform reasonably well. The direction of strains in second loading of test CID 2403 is predicted well with all models. But there are differences for first loading, in particular as mentioned before the isotropic model is not able to predict the development of deviatoric strains. In test CAE 2496, which was first loaded on extension side, the models using multilaminate framework and the SSC model slightly underestimate the strain gradient while S-CLAY1 overpredicts it. The direction of second loading is well predicted by all models.

In the last diagrams for each test the deviatoric strains are shown versus the deviatoric stress. There is no clear tendency observable for the S-CLAY1 model. In tests CAD 2261 and CAE 2496 the S-CLAY1 model overpredicts the deviatoric strains, whereas in tests CAD 2251 and CID 2403 the deviatoric strains are underpredicted. In contrast to that the other models mainly underpredict the test data. In the diagram for the test CID 2403, it is shown again, that the SSC model is not able to predict the development of deviatoric strains for first (isotropic) loading ( $\eta_1 = 0.0$ ).

Based on the simulations presented it is obvious that the differences between the multilaminate type models in comparison to the SCLAY1 model are small. Furthermore, there is not a very clear advantage of one anisotropic model over the others in comparison to the test results.

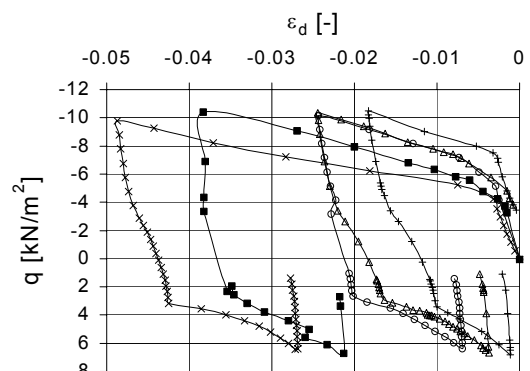
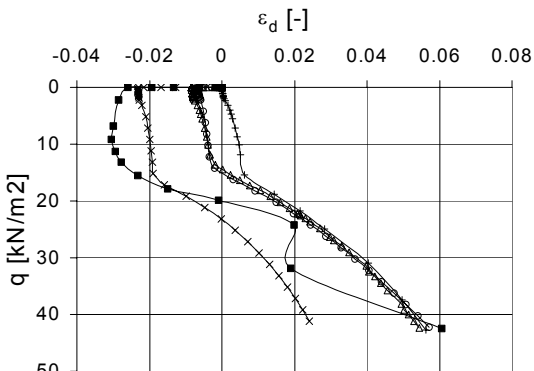
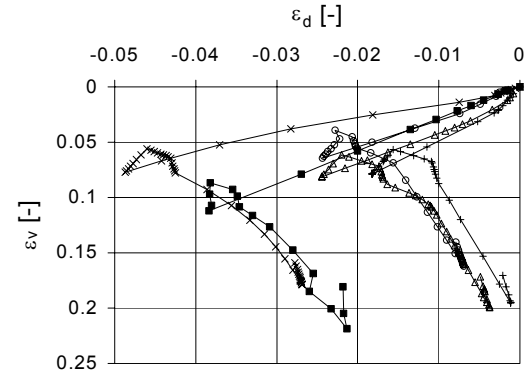
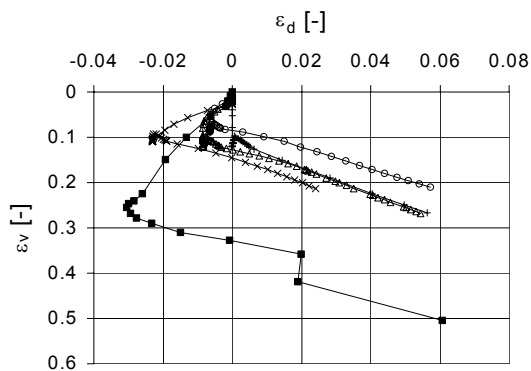
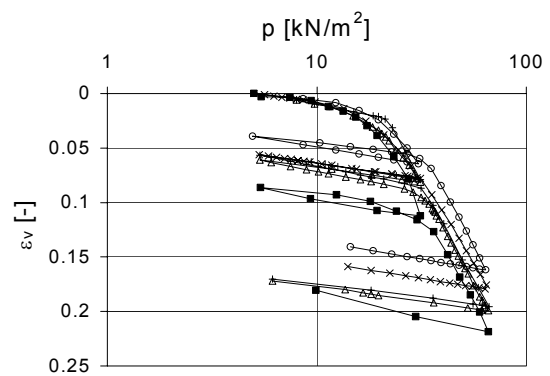
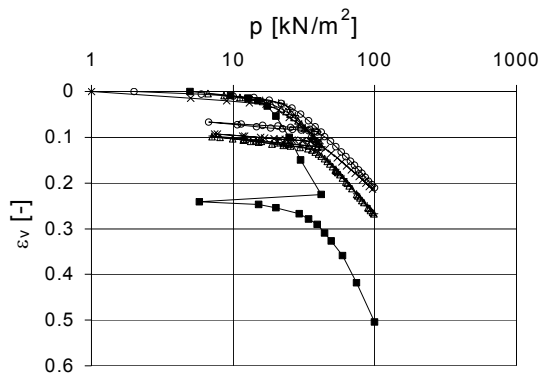


Figure 4. CID 2403 test results and simulations.

Figure 5. CAE 2496 test results and simulations.

#### 4 CONCLUSIONS

The performance of four different constitutive models simulating drained triaxial tests on a natural clay has been shown. The two different approaches of modelling anisotropy of clays (rotational hardening rule vs. multilaminate models) show no special advantages in comparison to each other. It is obvious that the isotropic model SSC has problems to predict the deviatoric strains correctly in all tests. The SSC model can predict volumetric strains equally well as the models with anisotropic formulations. Moreover, the models that take viscosity into account have no advantages in this case because of the chosen loading rates. Using a value of  $\lambda$  and  $\lambda^*$  corresponding to  $K_0$ -conditions instead of isotropic conditions would improve the prediction of volumetric strains for all models, but these would still be discrepant in the predicted and observed volumetric strains due to the effect

of destructuration that occurs at different rates for different stress paths. Experience suggests that the fit between observations and model predictions would be improved by accounting for destructuration. Examples of such models are S-CLAY1S that is an extension to S-CLAY1 (Koskinen, Karstunen & Wheeler 2002) and Multilaminate Model with Destructuration (Cudny 2003).

## ACKNOWLEDGEMENT

The research presented in this paper was carried out as part of a Research Training Network "Soft Clay Modelling for Engineering Practice" supported by the European Community through the specific research and technological development programme "Improving the Human Research Potential and the Socio-Economic Knowledge Base". The experimental programme was funded by the Finnish Academy (Grant no: 53936).

## REFERENCES

- Bazant, Z.P. & Oh, B.H. 1985. Microplane model for progressive fracture of concrete and rock. *J. of Engineering Mechanics ASCE* 11(4): 559-582.
- Cudny, M. 2003. Simple multi-laminate model for soft soils incorporating structural anisotropy and destructuration. In Vermeer, Schweiger, Karstunen & Cudny (Eds.), *Proc. of the Int. Workshop on Geotechnics of Soft Soils – Theory and Practice (the present proceedings)*. VGE.
- Messerklinger, S. 2001 Numerical modelling of anisotropy of soft clays. Diploma thesis, Graz University of Technology, Austria.
- Koskinen, M., Karstunen, M. & Wheeler, S.J. 2002. Modelling destructuration and anisotropy of a natural soft clay. In Mestat, Ph. (Ed.), *Proc. NUMGE02, Paris, France*: 11-20. Paris, Presses de l'ENPC/LCPC.
- Näätänen, A., Wheeler, S., Karstunen, M. & Lojander, M. 1999. Experimental investigation of an anisotropic hardening model for soft clays. *Proc. of the 2<sup>nd</sup> Int. Symp. on Pre-failure Deformation Characteristics of Geomaterials, Torino*: 541-548. Lisse, A.A. Balkema.
- Neher, H.P., Wehnert, M. & Bonnier, P.G. 2001. An evaluation of soft soil models based on trial embankments. In Desai et. al. (Eds), *Proc. of the 10<sup>th</sup> Int. Conf. on Computer Methods and Advances in Geomechanics (IACMAG), Tuscon*: 373-378. Rotterdam, A.A. Balkema.
- Neher, H.P., Vermeer, P.A. & Bonnier, P.G. 2001. Strain-rate effects in soft soils modelling and application. In Lee, C.F., Lau, C.K., Ng, C.W.W., Kwong, A.K.L., Pang, P.L.R., Yin, J.-H. & Yue, Z.Q. (Eds.), *Proc. of the 3<sup>rd</sup> Int. Conf. on Soft Soil Engineering, Hong Kong*: 361-367. Rotterdam, A.A. Balkema.
- Neher, H.P., Cudny, M., Wiltafsky, C. & Schweiger, H.F. 2002. Modelling principal stress rotation effects with multilaminate type constitutive models for clay. In Pande, G.N. & Petruszczak, S. (Eds), *Proc. of the 8<sup>th</sup> Int. Symp. Numerical Models in Geomechanics (NUMOG), Rome*: 41-47. Lisse, Swets & Zeitlinger.
- Pande, G.N. & Sharma, K.G. 1983. Multi-laminate model of clays - a numerical evaluation of the influence of rotation of principal stress axes. *Int. J. Numer. Anal. Meth. Geomech.* 7(4): 397-418.
- Pietruszczak, S. & Pande, G.N. 1987. Multi-laminate framework of soil models - Plasticity formulation. *Int. J. Numer. Anal. Meth. Geomech.* 11(6): 651-658.
- Roscoe, K.H. & Burland, J.B. 1968. On the generalised stress-strain behaviour of "wet" clay. *Engineering Plasticity*: 553-569. Cambridge University Press.
- Sterr, C. 2002. Numerische Modellierung der Anisotropie weicher Tone. Diploma thesis, University of Stuttgart, Germany.
- Toivanen, T.L. 1999. Modelling the anisotropy of Otaniemi Clay. Master's thesis, Helsinki University of Technology, Finland.
- Vermeer, P.A. 1978. A double hardening model for sand. *Géotechnique* 28(4): 413-433.
- Vermeer, P.A. & Neher, H.P. 1999. A soft soil model that accounts for creep. In Brinkgreve, R.B.J. (Ed.), *Proc. of the Int. Symp. "Beyond 2000 in Computational Geotechnics", Amsterdam*: 249-261. Rotterdam, A.A. Balkema.
- Wheeler, S.J., Näätänen, A., Karstunen, M. & Lojander, M. 2003. An anisotropic elastoplastic model for soft clays, *Can. Geotech. J.* 40: 403-418.
- Wiltafsky, C., Messerklinger, S. & Schweiger, H.F. 2002. An advanced multilaminate model for clay. In Pande, G.N. & Petruszczak, S. (Eds) *Proc. of the 8<sup>th</sup> Int. Symp. Numerical Models in Geomechanics (NUMOG), Rome*: 67-73. Lisse, Swets & Zeitlinger.
- Zienkiewicz, O.C. & Pande, G.N. 1977. Time-dependent multilaminate model of rocks - A numerical study of deformation and failure of rock masses. *Int. J. Numer. Anal. Meth. Geomech.* 1(3): 219-247.